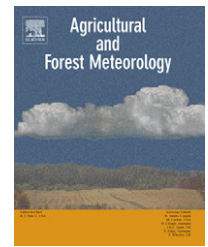




available at www.sciencedirect.com



journal homepage: www.elsevier.com/locate/agrformet Disponible en



Review

Estimation of live fuel moisture content from MODIS images for fire risk assessment

Marta Yebra ^{a,*}, Emilio Chuvieco ^a, David Riaño ^b

^a Department of Geography, University of Alcalá, Calle Colegios 2, Alcalá de Henares, Madrid 28801, Spain

^b Center for Spatial Technologies and Remote Sensing, U. California, Davis, CA, USA

ARTICLE INFO

Article history:

Received 15 January 2007

Received in revised form

6 December 2007

Accepted 8 December 2007

Keywords:

Remote sensing

Radiative transfer models

Fuel moisture content

Fire risk assessment

MODIS

ABSTRACT

This paper presents a method to estimate fuel moisture content (FMC) of Mediterranean vegetation species from satellite images in the context of fire risk assessment. The relationship between satellite images and field collected FMC data was based on two methodologies: empirical relations and statistical models based on simulated reflectances derived from radiative transfer models (RTM). Both models were applied to the same validation data set to compare their performance. FMC of grassland and shrublands were estimated using a 5-year time series (2001–2005) of Terra moderate resolution imaging spectroradiometer (MODIS) images. The simulated reflectances were based on the leaf level PROSPECT coupled with the canopy level SAILH RTM. The simulated spectra were generated for grasslands and shrublands according to their biophysical parameters traits and FMC range. Both models, empirical and statistical models based on RTM, offered similar accuracy with better determination coefficients for grasslands ($r^2 = 0.907$, and 0.894 , respectively) than for shrublands ($r^2 = 0.732$ and 0.842 , respectively). Although it is still necessary to test these equations in other areas with analogous types of vegetation, preliminary tests indicate that the adjustments based on simulated data offer similar results, but with greater robustness, than the empirical approach.

© 2007 Elsevier B.V. All rights reserved.

Contents

1.	Introduction	000
2.	Methods	000
2.1.	Field sampling	000
2.2.	MODIS data	000
2.3.	Generation of simulated reflectances	000
2.4.	Data analysis	000
3.	Results	000
3.1.	FMC evolution versus reflectance data	000
3.2.	Correlations between simulated reflectance and FMC	000
3.3.	Performance of empirical and simulation results	000

* Corresponding author. Tel.: +34 918855257; fax: +34 918854429.

E-mail addresses: marta.yebra@uah.es (M. Yebra), driano@ucdavis.edu (D. Riaño).

0168-1923/\$ – see front matter © 2007 Elsevier B.V. All rights reserved.

doi:10.1016/j.agrformet.2007.12.005

24
25 4. Discussion 000
26 5. Conclusions 000
27 Acknowledgements 000
References 000

28
29

81

30 **1. Introduction**

31 Wildfires are a natural disturbance worldwide, being respon- 82
32 sible for an important share of global greenhouse gas 83
33 emissions (Palacios-Orueta et al., 2005), land use change 84
34 (Ahern et al., 2001), and soil degradation (Doerr et al., 2006). 85
35 Fires also have positive feedbacks in the vegetation natural 86
36 succession and soil properties, but these effects are very much 87
37 dependent on fire intensity and duration (Johnson and 88
38 Miyanishi, 2001).

39 Mediterranean ecosystems have co-existed with fires for 89
40 millennia, since summer drought makes them prone to fire 90
41 ignition and therefore can be considered a natural phenom- 91
42 enon (Naveh, 1989). However, recently the natural fire regim- 92
43 en has changed, increasing the harmful effects of wildland fires, 93
44 both on environment and society. Climate change has not 94
45 been widely reported as a key issue in the changes in the 95
46 Mediterranean fire regime but land use changes as a result of 96
47 economic transition from agricultural to industrial societies 97
48 first, and then the increase in tourist-related land uses are 98
49 most commonly recognized as the main drivers of the recent 99
50 fire activity in the region (Vega-Garcia and Chuvieco, 2006). 100
51 Therefore, the growing urbanization of forested areas has 101
52 increased too the potential damage of fire on the wildland- 102
53 urban interface (Leone, 2003).

54 New strategies for earlier fire prevention and extinction are 103
55 required to handle these new threats and to improve the 104
56 management of the Mediterranean forests. Wildfire risk 105
57 evaluation systems provide an integrated approach for 106
58 managing resources at stake and reducing the negative 107
59 impact of wildland fires. These systems should include a 108
60 wide range of factors that are related to fire ignition, fire 109
61 propagation and fire vulnerability (Chuvieco et al., 2003b). Fuel 110
62 moisture content (FMC), defined as the proportion of water 111
63 over dry mass, has been the most extended measure of fire 112
64 ignition and fire propagation potential, and it has been widely 113
65 used for fire danger assessment (Blackmarr and Flanner, 1968; 114
66 Fosberg and Schroeder, 1971; Paltridge and Barber, 1988; 115
67 Pompe and Vines, 1966; Trowbridge and Feller, 1988; Viegas 116
68 et al., 1992), since the fuel water content has a clear impact on 117
69 ignition delay and fire rate of spread (Nelson, 2001). FMC is also 118
70 critical for planning of prescribed burns (Baeza et al., 2002) 119
71 which are growingly considered a critical aspect of integrated 120
72 fire management. Finally, it has also been related to burning 121
73 efficiency, which is a critical component of fire emission 122
74 models (Chuvieco et al., 2004a). In addition to fire-related 123
75 applications, the estimation of plant water content is an 124
76 essential input of vegetation productivity models (Boyer, 125
77 1995), and to improve water management in irrigated 126
78 agriculture (Sepulcre-Canto, 2006).

79 Direct estimation by field sampling provides the most 127
80 accurate method to obtain FMC, commonly using gravimetric 128
81 methods, namely the weight difference between fresh and dry 129

130 samples (Lawson and Hawkes, 1989). However, this approach 131
132 is very costly and the generalization to regional or global scales 132
133 results unfeasible. The use of meteorological indices is 133
134 widespread, since they provide an easy spatial and diachronic 134
135 estimation of FMC (Camia et al., 1999), but they also present 135
136 operational difficulties since the weather stations are often 136
137 located far from forested areas and may be scarce in fire prone 137
138 regions. Furthermore, these estimations are reasonably well 138
139 suited for dead fuels, because their water content is highly 139
140 related to atmospheric conditions. However, in live fuels, 140
141 species physiological characteristics and adaptation to 141
142 drought imply a great diversity of moisture conditions with 142
143 the same meteorological inputs (Viegas et al., 2001).

144 FMC estimation of live fuels can also be based on remote 143
145 sensing methods, since FMC variations affect fuel reflectance 144
146 and temperature. The monitoring of grass curing from satellite 145
147 images was proposed by Burgan and collaborators (Burgan and 146
148 Hardy, 1993), within the potential revisions of the National Fire 147
149 Danger Rating System (NFDRS). A further elaboration of this 148
150 concept led to the use of greenness indices (defined as the 149
151 relative change in vegetation index values with respect to time 150
152 series maximum and minimum) as an estimation of dead 151
153 versus live fuels proportion to compute fire danger potential 152
154 (Burgan et al., 1998). Later, both empirical (Chen, 2005; 153
155 Chuvieco et al., 2004b; Paltridge and Barber, 1988; Roberts 154
156 et al., 2006) and simulation approaches (Jacquemoud and 155
157 Ustin, 2003; Riaño et al., 2005; Zarco-Tejada et al., 2003) were 156
158 developed to estimate FMC from remote sensing data. The 157
159 empirical methods are commonly based on statistical fitting 158
160 between field-measured FMC and reflectance data. They have 159
161 a known accuracy and are simple to compute. However, those 160
162 empirical relationships are sensor and site-dependent, and 161
163 therefore difficult to extrapolate to regional or global scale 162
164 studies due to differences in leaf and canopy characteristics 163
165 (Riaño et al., 2005) or sensor calibration and observation 164
166 conditions. 165

167 Estimation of water content from simulation approaches 166
168 has frequently been based on inversion of radiative transfer 167
169 models (RTM). Since these models are based on physical 168
170 relationships that are independent of sensor or site condi- 169
171 tions, they should be more universal than empirical fittings. 170
172 However, the selection and parameterization of RTM is far 171
173 more complex than empirical models, since they are based on 172
174 assumptions that may not accurately resemble those found in 173
175 nature, especially when complex canopies are involved (Liang, 174
176 2004). Most studies based on RTM have found that the 175
177 equivalent water thickness (EWT), defined as the amount of 176
178 water per leaf area, can be retrieved from reflectance data, 177
179 since it represents the water absorption depth of leaves 178
180 (Ceccato et al., 2002; Datt, 1999). However, the FMC is more 179
181 difficult to estimate from reflectance measurements, since it 180
182 does not only depend on water absorption, but also on the 181
183 changes in dry matter as a result of leaf drying. Sensitivity 182
184

81
82
83
84
85
86
87
88
89
90
91
92
93
94
95
96
97
98
99
100
101
102
103
104
105
106
107
108
109
110
111
112
113
114
115
116
117
118
119
120
121
122
123
124
125
126
127
128
129
130
131
132
133
134

analysis based on a wide range of conditions has found potential for FMC retrieval from reflectance measurements (Bowyer and Danson, 2004), providing that the dry matter content can also be estimated (Riaño et al., 2005).

The main objective of this study was to compare the performance of empirical and RTM approaches to derive FMC of Mediterranean species from satellite reflectance measurements. The final goal was to derive an operational estimation that could be integrated with other factors of wildland fire risk.

2. Methods

The general scheme of the method developed in this paper is presented in Fig. 1. The empirical approach was derived from multivariate linear regression (MLR) analysis between field-collected FMC data and reflectance values derived from the moderate resolution imaging spectroradiometer (MODIS). The field samples were divided in two sets: 60% for calibrating the model and the remaining 40% for the validation. Two different models were built for grasslands and shrublands. The simulation approach was derived from RTM that were parametrized using field data, auxiliary information derived from MODIS products and the knowledge of the type of canopy architecture that define which RTM is appropriate (Combal et al., 2002). Once the simulated reflectance values for grasslands and shrublands were obtained for the whole solar spectrum, they were convolved to the MODIS spectral wavelengths and band widths. Finally, separate MLR models between the simulated reflectances and the grassland and shrubland FMC values were built, in a similar way to the

empirical method. Those equations were applied to the MODIS data for the same validation dataset as the empirical model to compare the performances of both approaches.

2.1. Field sampling

A field campaign has been carried out by our research group since 1996 to the present in the Cabañeros National Park (Central Spain; Fig. 2) to collect samples of different Mediterranean species for field FMC estimation. Three plots of grassland and two of shrubland (*Cistus ladanifer* L., *Rosmarinus officinalis* L., *Erica arborea* L. and *Phyllirea angustifolia* L.) sized 30 m × 30 m, were collected in gentle slopes (<5%) and homogeneous patches. For this paper, FMC values of *C. ladanifer* L. were selected as representative for shrubland plots since it is very common in Mediterranean siliceous areas. It appears in a 29.79% of the study area covering a radius of 100 km from the National Park being the dominant species in more than 6% versus less than 16% of appearance and 1% of dominance of the other three species together in the same area. In addition to this, it is a typical pioneer species that regenerates easily by seeds after diverse types of handlings and disturbances (Nuñez Olivera, 1988), so it is the primary colonizer in areas with recurrent wildfires, which are of special interest in this study.

The sampling protocol followed standard methods described in Chuvieco et al. (2003a) and was repeated every 8 days during the spring and summer seasons from 1996 to 2002 and every 16 days from 2003 on. For this paper, FMC measurements taken from 2001 to 2005 have been used to correspond with the temporal series of the MODIS images.

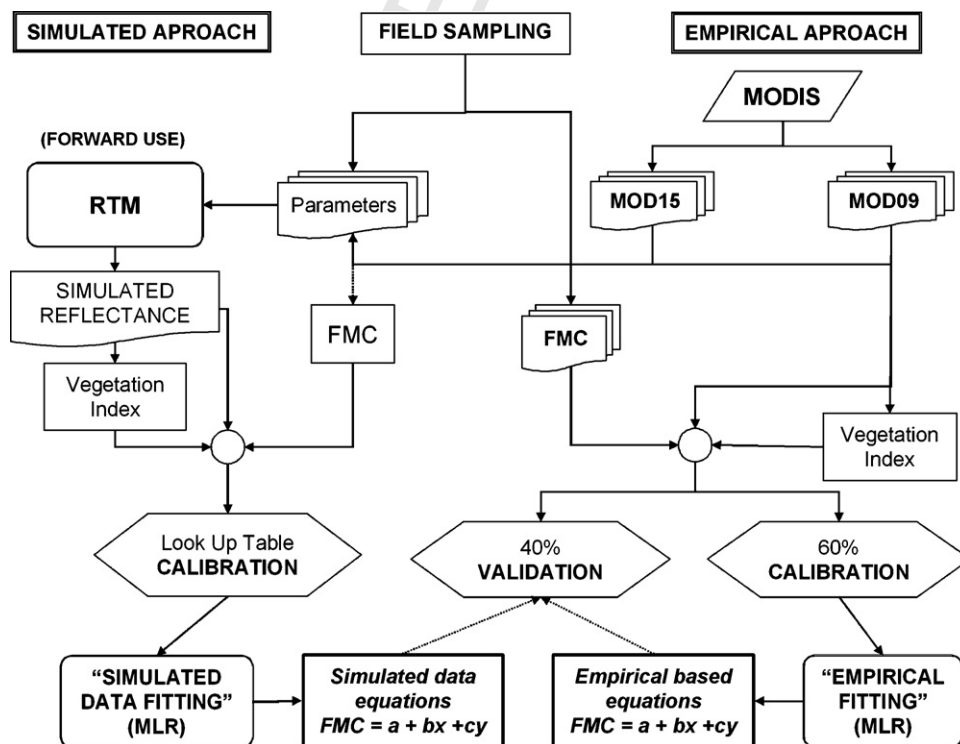


Fig. 1 – Methodological flowchart.

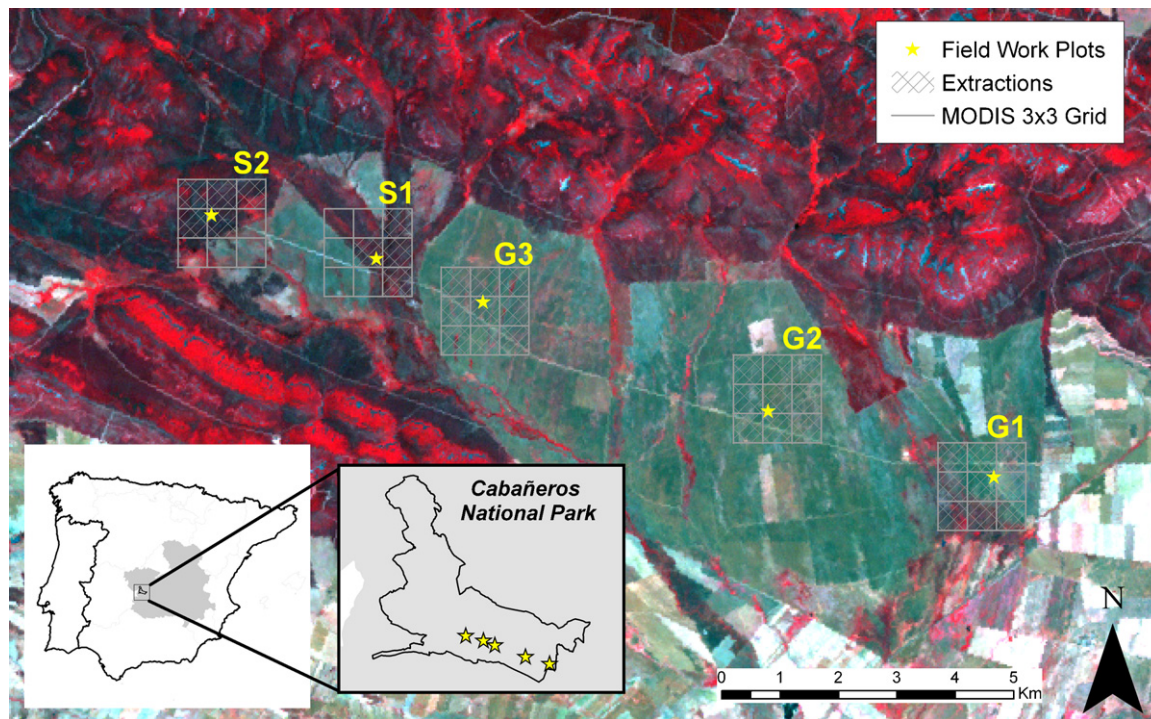


Fig. 2 – Map of Spain showing the location of Cabañeros National Park, as well as a false color composite Landsat image showing the midpoint of the shrubland (S1 and S2) and grassland (G1, G2 and G3) plots used in this analysis. The grey boxes indicate the 3×3 MODIS grid ($1.5 \text{ km} \times 1.5 \text{ km}$) centered at the plots. Shaded boxes indicate the window adapted to the shrub shape plot.

FMC was computed from the difference of fresh and dry weight as following:

$$\text{FMC (\%)} = \frac{W_f - W_d}{W_d} \times 100; \quad (1)$$

where W_f is fresh weight of leaves and small terminal branches (in the case of shrub species) or the whole plant (in the case of grassland), and W_d is dry weight, after oven drying the samples for 48 h at 60°C .

After 2004, FMC field sampling incorporated the collection of variables that are critical for running the RTM at leaf level, such as dry matter content (DM), equivalent water content (EWT) and chlorophyll content (Ca + b).

DM and EWT were computed following:

$$\text{DM (g cm}^{-2}\text{)} = \frac{W_d}{A}, \quad (2)$$

and

$$\text{EWT (g cm}^{-2}\text{)} = \frac{W_f - W_d}{A} \quad (3)$$

where W_f and W_d are the same as in (1) and A is the leaf area.

C. ladanifer L. leaf area was measured with an image analysis Delta system (Delta Devices LTD, Cambridge, England). Ca + b was measured by means of destructive sampling and measurement of leaf concentration in laboratory with the dimethyl sulfoxide (DMSO) method and spectrophotometric readings, according to Wellburn (1994). For grasslands, DM and

Ca + b measurements were provided by a field ecologist working in similar environments (Valladares, personal communication). Spectral soil reflectance was also measured with a GER 2600 (GER Corp., Millbrook, NY) radiometer to use as an input at canopy level model.

2.2. MODIS data

Two standard products of the MODIS program were chosen for this study: the MODIS/Terra surface reflectance (MOD09A1) and the MODIS/Terra leaf area index (LAI) and fraction of photosynthetically active radiation (FPAR) (MOD15A2). The first is an 8-day composite product of atmospherically corrected reflectance for the first seven spectral bands of the MODIS sensor at a spatial resolution of 500 m (Fig. 3). This product includes ancillary information, such as sun and sensor angles (Vermeulen and Vermeulen, 1999). The standard MOD15A2 product was selected to take into account the strong effect of LAI variations on reflectance as well as to parametrize the RTM. This product is generated daily at 1 km spatial resolution and composited over an 8-day period based on the maximum value of the FPAR for that period (Knyazikhin, 1999).

The original products were downloaded from the Land Processes Distributed Active Archive Center (LP DAAC) of the United States Geological Survey (USGS) (<http://edcimswww.cr.usgs.gov/pub/imswelcome/>) and reprojected from sinusoidal to UTM 30 T Datum European 1950 (ED50) using nearest neighbour interpolation resampling. MOD15A2 data were resampled to 500 m to match the resolution of the MOD09A1 product using the same interpolation algorithm. The values of a

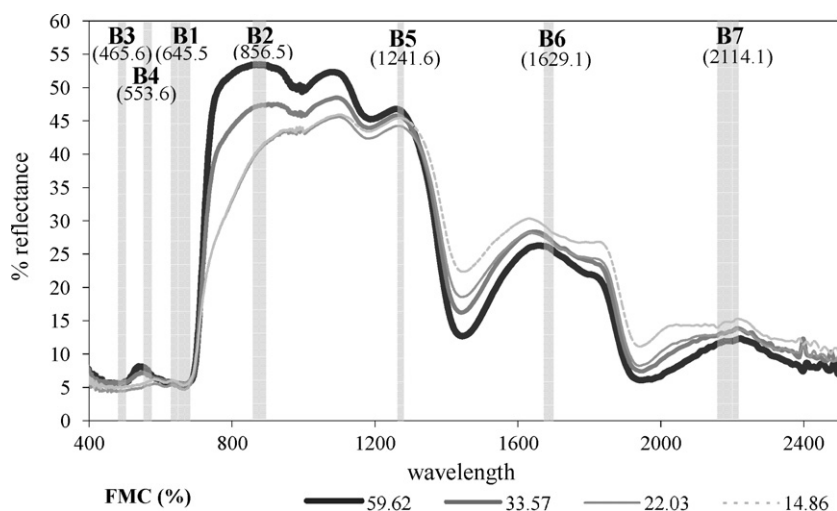


Fig. 3 – Example of reflectance spectrum (400–2500 nm) of different FMC values for *C. ladanifer* L. measured with GER 2600 under laboratory experimentation showing location of MOD09A1 band regions (grey bands) with their central wavelength (between brackets).

243
 244 given plot for comparing with the field data were extracted
 245 from each composited image using the median value of a
 246 3 × 3 pixel kernel located at the center of the field plot. A 3 × 3
 247 window was used in order to reduce the potential noise due to
 248 residual atmospheric effects and georeferencing errors. In the
 249 case of shrublands, extraction windows were adapted to the
 250 shape of shrub patches to avoid including mixed pixels (Fig. 2).
 251 To verify this approach the coefficient of variation (CV) was
 252 computed for reflectances for a Landsat image (30 m × 30 m
 253 pixel size) within the extraction windows. The CV decreased
 254 from 0.052 and 0.255 of the 3 × 3 windows in the near infrared
 255 band (NIR) and the short wave infrared (SWIR) bands,
 256 respectively, to 0.050 and 0.195 with the adapted window.
 257 The extractions of reflectance data of each pixel were derived
 258 from the 8-day composite that had a closest selected day to the
 259 field collections.

260 A wide range of vegetation indices were calculated to be
 261 included as independent variables in the empirical MLR model

(Table 1). Only one form of the NDII using band 6 (1628–
 262 1652 nm) was calculated based on previous studies which
 263 show stronger correlations between this band and field
 264 measured FMC values than other MODIS bands in the SWIR
 265 region (Roberts et al., 2006; Yebra et al., 2005).
 266

The first five indices in Table 1 measure greenness
 267 variations, which are only indirectly related to leaf water
 268 content. The other indices included in Table 1 are more
 269 directly related to water content, by combining water
 270 absorption in the SWIR wavelengths with other bands that
 271 are insensitive to water content (Fourty and Baret, 1997).
 272 Although greenness indices do not include water absorption
 273 bands, they can be used as an indirect estimation of water
 274 content, since moisture variations affect chlorophyll activity,
 275 leaf internal structure and LAI of many Mediterranean plants
 276 (Bowyer and Danson, 2004). In this sense, as the plant dries,
 277 changes in leaf internal structure cause a decrease in the
 278 reflectance in the NIR and an increase in the visible region, as a
 279

Table 1 – Spectral indices calculated for MODIS including their shortened acronym, mathematical formulation and citation

Index	Formula	Reference
“Normalized Difference Vegetation Index”	$NDVI = \frac{\rho_2 - \rho_1}{\rho_2 + \rho_1}$	(Rouse et al., 1974)
“Soil Adjusted Vegetation Index”	$SAVI = \frac{\rho_2 - \rho_1}{\rho_2 + \rho_1 + L} (1 + L)$	(Huete, 1988)
“Enhanced Vegetation Index”	$EVI = \frac{2.5(\rho_2 - \rho_1)}{\rho_2 + 6\rho_1 - 7.5\rho_3 + 1}$	(Huete et al., 2002)
“Global Environmental Monitoring Index”	$GEMI_i = \frac{\rho_1 - 0.125}{1 - \rho_1}$ $eta = \frac{2(\rho_2^2 - 1.5\rho_2 + 0.5\rho_1)}{\rho_2 + \rho_1 + 0.5}$	(Pinty and Verstraete, 1992)
“Visible Atmospheric Resistant Index”	$VARI_i = \frac{\rho_4 - \rho_1}{\rho_4 + \rho_1 - \rho_3}$	(Gitelson et al., 2002)
“Normalized Difference Infrared Index”	$NDII_6 = \frac{\rho_2 - \rho_6}{\rho_2 + \rho_6}$	(Hunt and Rock, 1989)
“Normalized Difference Water Index”	$NDWI = \frac{\rho_2 - \rho_5}{\rho_2 + \rho_5}$	(Gao, 1996)
“Global Vegetation Moisture Index”	$GVMI = \frac{(\rho_2 + 0.1) - (\rho_6 + 0.02)}{(\rho_2 + 0.1) + (\rho_6 + 0.02)}$	(Ceccato et al., 2002)

279 result of reducing photosynthetic activity and LAI values.
280 However, this relation cannot be generalized for all ecosys-
281 tems because, for example, variations on chlorophyll content
282 can also be caused by plant nutrient deficiency, disease,
283 toxicity and phenological stage (Ceccato et al., 2001).
284

2.3. Generation of simulated reflectances

285 The use of RTM in remote sensing analysis can follow two
286 different approaches: forward and backward simulation. The
287 former is based on changing input parameters and analyzing
288 the effects on the simulated reflectance to assess the
289 importance of each input parameter in the different spectral
290 wavelengths. The backward simulation, also named inver-
291 sion, estimates which set of input parameters produces a
292 simulated reflectance more similar to a particular observed
293 reflectance. The concept of “similar” spectrum is commonly
294 formalized in RTM inversion approaches using the merit
295 function, which implies minimizing the differences between
296 the observed and modeled reflectances:
297

$$\chi^2 = \sum_{i=1}^n [\rho_i - M(\Theta, X_i)]^2 \quad (4)$$

298 where χ is the difference between the observed reflectance (ρ)
299 and the modeled reflectance $M(\Theta, X)$, for a certain set of input
300 parameters (Θ, X), being X the value to be estimated, and n the
301 number of spectral wavelengths of the input image.
302
303

304 The inversion process can be achieved through iteratively
305 running the model until finding a spectrum (and its corre-
306 sponding set of parameters) that closely matches the
307 reflectance values extracted from satellite data. Alternatively,
308 the model can be run in advance and which of the simulated
309 reflectances is more similar to the observed spectrum can be
310 determined later. In both cases, once the most similar
311 simulated spectrum is found, the set of parameters that
312 generated that spectrum is considered a good estimation of
313 vegetation conditions of the area where that satellite
314 observation came from (Zarco-Tejada et al., 2003).

315 The second approach is usually designed as the generation
316 of a look up table (LUT) (Liang, 2004), and it is the most
317 commonly used since it is quicker, provides a control scenario
318 on the input parameters to be searched for (Combal et al., 2002)
319 and allows the identification of ambiguous situations where
320 there are several set of input parameters which can produce a
321 modeled result that agrees with the observations within a
322 tolerance (Gobron et al., 2000; Saich et al., 2003).

323 The LUT approach was selected for this paper. A LUT
324 includes the output of running the RTM for the different
325 simulation scenarios ($M(\Theta, X)$ as stated in (4)). Therefore, the
326 inversion process does not need to run the model for each
327 pixel of the image, but rather it can focus on finding which of
328 the modeled spectrum is most similar to an observed pixel
329 reflectance, most commonly using a merit function of
330 “spectral similarity” based on the quadratic distance (as
331 formulated in (4)). Alternatively to this search, relationships
332 over the modeled spectrums and a corresponded key
333 biophysical parameter, using neural network or genetic
334 algorithms (Fang and Liang, 2003) can be built. For this study,
335 a MLR between the simulated reflectance and their associate

335 FMC in the LUT was used, in a similar way as the model
336 derived for empirical data.
337

338 Spectral reflectances between 400 and 2500 nm were
339 simulated for different FMC values by linking two well-known
340 RTM: the PROSPECT leaf model (Jacquemoud and Baret, 1990)
341 and the SAILH canopy model (Verhoef, 1984). PROSPECT
342 simulates reflectance and transmittance of a leaf by consider-
343 ing it as a set of N stacked layers with several absorption
344 components ($C_a + b$; DM and EWT). SAILH is a model that
345 simulates canopy reflectance from the output of the PRO-
346 SPECT model (leaf reflectance and transmittance) plus a set of
347 variables affecting the canopy. The main ones are the leaf area
348 index (LAI), leaf angle distribution function (LADF), the hotspot
349 parameter, which is a relation between leaf size and canopy
350 height, the soil substrate (soil reflectance) and viewing and
351 illumination conditions (Sun and view zenith angle, relative
352 azimuth sensor-sun angle and atmospheric transmissivity).

353 The PROSPECT–SAILH models were run to create a LUT for a
354 wide set of FMC values. For each simulation case, the FMC was
355 computed as a ratio of EWT and DM, two of the input
356 parameters of the PROSPECT model. Input parameters for
357 running these models are included in Table 2. They were
358 derived from our field sampling and literature review. A
359 random noise factor of the size of half a step of the simulation
360 was introduced in the simulation step to cover the variation
361 space of the model and therefore avoid gaps with fixed values.

362 Since the set of simulations might include unrealistic
363 combinations of input parameters, a filter criterion was
364 applied to eliminate those simulations which would not be
365 likely to occur. In Mediterranean conditions, annual grasses
366 escape drought by reducing their vital cycle and when grass
367 dries it tends to reduce leaf cover as a result of losing turgidity
368 and the consequent leaf curling (Valladares, 2004). On the
369 other hand, shrubs frequently adapt to the summer condition
370 by reducing leaf area and increasing non-photosynthetic
371 material (Valladares, 2004), and therefore increasing DM. For
372 all above mentioned, either the lowest LAI or highest DM
373 values are unlikely to combine with the highest FMC in
374 Mediterranean grasslands or shrublands, respectively. There-
375 fore, field observations were used to derive two linear
376 relations, a positive one between FMC and LAI for grasslands,
377 and another negative between FMC and DM for shrublands
378 (Fig. 4) and were used for filtering out some of the simulations.
379 The cases that exceeded a 10% of the maximum or minimum
380 residual of the regression fitting were eliminated. This 10%
381 margin of error was arbitrary added in order to take into
382 account the possibility that other sites, with other species,
383 have different relations. It must be better determined by
384 measurements at other sites.

385 The final LUT included 1331 spectra for grasslands and 503
386 for shrublands. The simulated spectra were convolved to the
387 seven MOD09A1 reflectance bands, by means of sensor
388 response functions, to be used as input bands for the MLR
389 model. Additionally, the same vegetation indices considered
390 in the empirical model were computed as well (Table 1).

2.4. Data analysis

391 The empirical modeling was based on stepwise multivariate
392 linear regression analysis (MLR). Forward inclusion with 0.08
393

Table 2 – Input parameters for the PROSPECT-SAILH simulations

Model	Parameter	Grassland			Shrubland		
		Min.	Mx.	Step	Min.	Mx.	Step
Prospect	N	1.25	2.5	0.5	1.25	2.5	0.5
	DM (g cm ⁻²)	0.002	0.007	0.001	0.02	0.04	0.003
	EWT (g cm ⁻²)	0.0001	0.017	0.0003	0.012	0.03	0.002
	Ca + b (μg cm ⁻²)	20	20	-	45	45	-
Sailh	LAI	0.5	2	0.6	0.5	3	0.6
	Hotspot	0.001	0.001	-	0.008	0.008	-
	ts	27	51	16	27	51	16
	tv	5	5	-	5	5	-
	psr	-30	-30	-	-30	-30	-

SAILH LADF parameter was fixed to erectophile and plagiophile for grasslands and shrublands, respectively. The soil spectrum was that one measured in Cabañeros National Park. Sun zenith angle (ts), sensor zenith angle (tv), and relative azimuth sensor-sun (psr) in degrees.

(in) and 0.1 (out) significance levels were selected (SPSS, 2004). Two different models were used for FMC estimation, one for grasslands and one for shrub species, using *C. ladanifer* L. as a representative species. Average values of the three plots of grasslands on one hand, and the two plots of *C. ladanifer* L. on the other, were used for building the models. In this way, the FMC values are more representative of the coarse pixel size of the MODIS images. There were 66 sample periods, which were

randomly divided into two groups, 60% for the calibration of the empirical models (n = 40) and 40% for the validation (n = 26). To check the robustness of the relationships, several 60% random samples were obtained to derive the linear models. Dry and wet years were included in each group, which assures greater significance of the results.

Two additional linear regression models for grassland and shrublands were built with the simulated reflectance and FMC

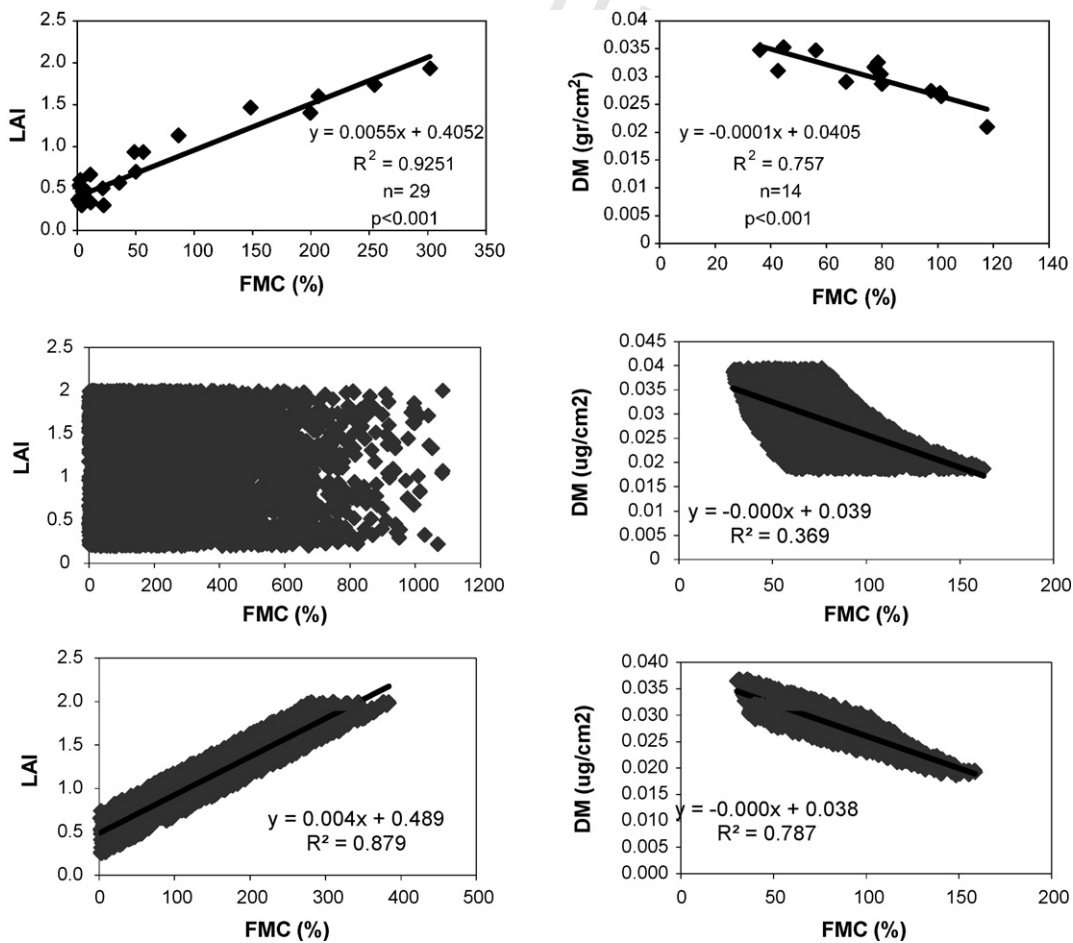


Fig. 4 – Scattergraphs of relations between FMC and LAI (grasslands), and DM (shrubland) for field data observations (top), initial LUT (center) and final LUT (bottom). These models were derived exclusively from field data, only periods with LAI and DM field data were considered.

values using stepwise forward MLR selection. Model calibration for each vegetation class was based on all of the simulated dataset so in this case the sample was much higher than for empirical data, since there were many more simulations than field sampling periods. To better compare results with the empirical data, the validation of these models was performed with the same cases used to assess the empirical models. In this case, the independent variables for the MLR were the MODIS simulated reflectances, the spectral indices derived from them (extracted from the LUT) as well as the LAI values for the grassland model and the DM values for the shrublands model. The decision to include LAI and DM in the MLR analysis was based on previous experience with RTM iterative inversion software (Rueda, 2001), which only offered good results when LAI and DM were fixed. In this sense, if the FMC models are calibrated using LAI or DM as independent variables they will account for variation in these two parameters and ancillary data can be used later on to fix those values, in the same way that they were fixed in the iterative algorithm, and therefore the inversion is constrained.

For the validation with the same sample as the empirical models, the LAI values were extracted from the MODIS standard LAI product (MOD15A2), and the DM was estimated from our seasonal field measurements. As a starting approach a simple model based on just two average DM values for spring (0.026 g cm^{-2}) and summer (0.032 g cm^{-2}) were used. Similarly to the empirical approach, once the model was calibrated, several 60% random samples were obtained to check the robustness of the relationships.

The accuracy of the empirical and simulated models was measured from the determination coefficient (r^2), the slope of the relationship between observed and predicted values and the root mean square error (RMSE), which summarize the difference between the observed and predicted FMC. This RMSE was decomposed into systematic (RMSEs) and unsystematic (RMSEu) portions (Willmott, 1982). The latter takes into account errors caused by uncontrolled factors, while the former considers errors caused by the model performance and the predictors included. A good model is considered to have an RMSEu much larger than the RMSEs.

3. Results

3.1. FMC evolution versus reflectance data

Temporal trends in FMC values and several MODIS bands are shown in Fig. 5. FMC values of grasslands show a large oscillation between the spring and summer seasons. The former had values in the range of 250–300%, while the latter presented FMC values below 30%, which can be considered as dead matter. This cycle in FMC values was clearly observed too in the MODIS reflectance data, although with maximum FMC values corresponded with minimum reflectance values in the band 1 (620–670 nm), 6 (1628–1652 nm) and 7 (2105–2155 nm) wavelength, and maximum in band 2 (841–876 nm). The spring/summer variation of FMC values in 2005 was lower than in other years, because of the exceptional dry conditions. However, the reflectance variation is similar to other years, with the exception of band 2, which shows an increase in

reflectance instead of a decrease in summer time. The reflectance values of April 2005, practically match those FMC values at the beginning of June for the rest of the years.

Less seasonal oscillation is observed for FMC values of shrublands, which range between 60% and 120% most years. The exception is again 2005 with very low FMC values. That year, the FMC contents were below 100% in the spring season, reaching values below 60% in summer time. FMC had similar effects on reflectance bands 1, 6 and 7 as in the grassland case but seasonal reflectance variations, just like FMC one, were much smaller in amplitude. These lower variations were reflected in the regression analyses that follow. For shrublands, NIR band (2) did not show a clear correspondence to FMC variations.

Table 3 shows Pearson r coefficients between the temporal evolution of FMC and MODIS reflectance bands. Bands 1, 6 and 7 had significant correlations both for grasslands ($p < 0.001$) and shrublands, although in this case with lower significance level ($p < 0.005$). Band 2 was significant for grassland ($r = 0.54$, $p < 0.001$) while it was uncorrelated with shrubland FMC ($r = 0.0078$). The spectral vegetation indices showed very good correlations for grasslands ($r > 0.62$), and lower for shrublands ($0.32 < r < 0.81$). The red/NIR indices (EVI, NDVI, SAVI) provided a sound estimation of FMC for grasslands, while those based on the NIR/SWIR space (NDII, GVMI, NDWI) offered better results for shrublands, although NDVI still provides high r values for shrublands. The VARI index, which is a combination of the blue–green–red reflectance, provided the best correlation for *C. ladanifer*, but offered the lowest for grasslands, being the only index with higher correlations for shrubs than for grasslands.

3.2. Correlations between simulated reflectance and FMC

The highest coefficients were observed for those bands located in the SWIR (bands 6 and 7, Table 3). Bands 1 (red) for grassland and 2 (NIR) for shrublands had also a high r coefficient. The latter was opposite to the empirical data, which did not show a significant relationship for band 2. Band 5 (1230–1250 nm) offered better correlations for the simulated than for the observed reflectances. Similarly to the empirical approach, shrubland correlations were generally lower than for grasslands. The spectral indices computed for simulated data provided similar results as those observed for empirical data, although the performance of red/NIR indices for grasslands was less important than for the indices based on the NIR/SWIR. Contrary to the empirical data, the VARI worked better for grasslands than for shrublands.

3.3. Performance of empirical and simulation results

Table 4 shows the variables selected for the MLR empirical models with the different random samples selected. For models derived from empirical data, NDVI was always selected as the most explicative variable for grasslands, and accounted for almost 90% of input variance. The r^2 determination coefficients were similar in the four runs of the model, but the slopes and constants of the equations as well as the standard errors of the estimation (S.E., standard deviation of the error) changed. The selected model (identified as 0 in

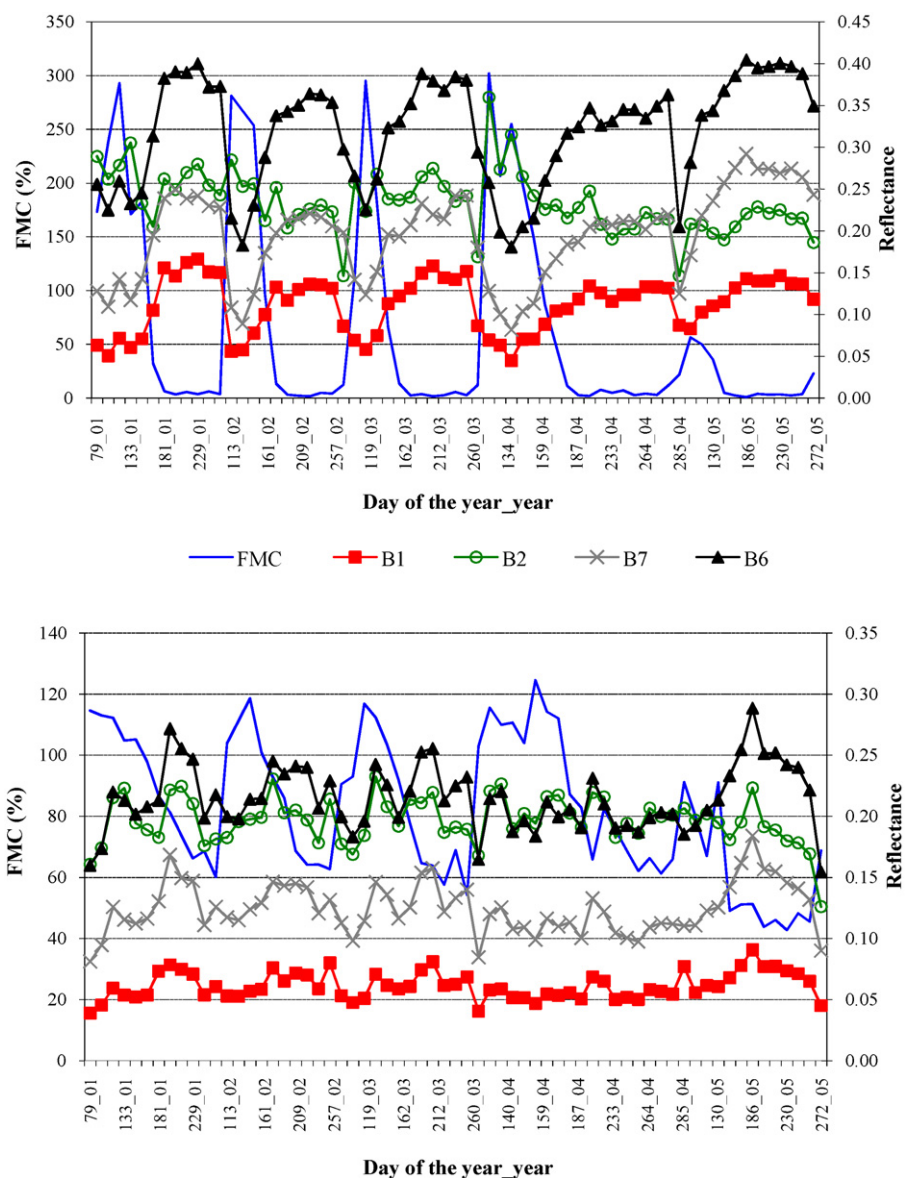


Fig. 5 – Temporal evolution of FMC and MODIS bands 1, 2, 6 and 7 reflectance in the study area for grasslands (top) and shrublands (bottom).

Table 4) had an S.E. of 30.1%. For shrublands, the r^2 determination coefficients of the MLR estimations were lower than for grasslands, with values between 0.67 and 0.73. The S.E. of the calibrated model was 17.5%. Variables selected were VARI and GVMI, the former accounted for most of the explained variance. As in the case of grasslands, the differences in models by varying randomly the input cases were clearly observed, with notable changes in slopes, constant and S.E.

Models derived from the simulation data show a different behaviour from those generated from empirical data (Table 5). The selected variables were in greater correspondence with the spectral water absorption features. For grasslands, the LAI and the NDII values were selected, but not the NDVI or other red/NIR index. For the shrublands, DM PROSPECT parameter and GVMI were selected. It was observed that choosing

randomly 60% cases for the calibration produced slight changes in the models (Table 5). Total determination coefficients were similar to the models generated from empirical data, but standard errors were lower for both grassland (29.5%) and shrubland (12.6%).

The validation of the empirical and simulated data models was carried out with the remaining 40% of the field-FMC measures. In this case, the model inputs were MODIS reflectances in both the empirical and the simulated model, since the simulation was only used to calibrate the model, but the validation was performed with real data. This was also the case for the LAI and DM values, as previously mentioned.

Similar determination coefficients were found for the empirical and simulated data model in both grassland and shrublands (Table 6). The RMSE of the grassland model was higher for the empirical than for the simulated data but the

Table 3 – Pearson correlation coefficients between FMC and MODIS-derived data for simulated (SIM) and observed (OBS) data

Pearson	Grassland		Shrubland	
	FMC _{OBS}	FMC _{SIM}	FMC _{OBS}	FMC _{SIM}
B3	-0.725	-0.621	<u>-0.428</u>	-0.431
B4	-0.680	-0.195	-0.328	-0.169
B1	-0.816	-0.710	-0.532	-0.440
B2	0.540	0.215	0.078	0.698
B5	-0.241	-0.637	-0.226	-0.197
B6	-0.768	-0.799	<u>-0.421</u>	-0.552
B7	-0.771	-0.793	<u>-0.427</u>	-0.503
NDII ₆	0.887	0.902	0.606	0.710
NDWI	0.859	0.915	0.482	0.751
GVMi ₆	0.890	0.887	0.604	0.688
EVI	0.945	0.721	0.421	0.760
GEMI	0.896	0.554	0.324	0.772
VARI	0.623	0.812	0.810	0.517
NDVI	0.952	0.792	0.678	0.590
SAVI	0.933	0.788	0.541	0.645
Samples, n	40	2270	40	503

Bold numbers refer to significant correlations at $p < 0.001$. Underlined are significant at $p < 0.005$.

ratio of estimated versus observed FMC values (slope) was quite similar and close to 1 for both generated grasslands models. These RMSE values were computed after negative estimations, which may occur during the driest periods of the summer season, were removed. The RMSEu portion of the residual error was higher than the RMSEs for both simulated and empirical datasets. Regarding the shrublands, the empirical data-derived model showed a closer to 1 slope and a lower RMSE than the model derived from the simulated. This later model has a RMSEs higher than the RMSEu.

Fig. 6 shows the temporal trends observed and estimated for the two different models in both grasslands and shrublands. Both the empirical and simulated data model provide better fittings for grasslands variation than for shrublands, where tendencies to overestimation (empirical data model) and underestimation (simulated data model) were observed, especially during the summer period. In the driest year of our study series (2005) grasslands FMC was poorly estimated by the empirical model, while the model based on simulation data was closer to measured values in the spring season (day 111). On the contrary, from the later spring (day 130) onwards, the empirical model performed better than the simulated data model.

4. Discussion

This paper has compared the performance of empirical versus simulated reflectance data for estimating live FMC values. The pros and cons of each approach may be summarized in Table 7. Empirical models, which have been extensively used in remotely sensed applications, generally provide an accurate estimation of the target variable, but are very costly to generate and have only local application. In the case of FMC estimation, empirical models can be generalized by using a wider set of input data, but it would imply an extensive field sampling effort.

Estimations based on simulated data from RTM are a sound alternative to empirical approaches, providing a more physical basis to understand observed relationships. However, they are difficult to parameterize and have assumptions that are not always found in nature. They also present uncertainties in the inversion mode, since very similar reflectances can be derived from a different set of input parameters, which is the well-known ill-posed inverse problem (Garabedian, 1964). Additionally, the physical models do not take into account ecophysiological relations, and therefore they might provide poor estimations when unrealistic combinations of input parameters are considered. Finally, the noise associated with the sensor and data processing (radiometric calibration and atmospheric correction) and illumination effects increase the uncertainties of the inversion process (Combal et al., 2002).

This paper has shown a simple inversion technique based on MLR to retrieve FMC from MODIS data. This estimation has been compared to traditional empirical models in terms of accuracy and robustness.

The Pearson coefficient analysis between FMC values and vegetation indices carried out before the MLR analysis showed that all the red/NIR indices except GEMI correlated with grasslands FMC stronger than NIR/SWIR. This might be due to the fact that GEMI breakdowns with respect to soil noise at low vegetation covers (Qi et al., 1994), which occurs mainly on summer time. On the other hand, NDVI was the only red/NIR index which correlated with shrubs FMC practically the same as GVMi and NDII, and higher for NDWI. The former was no expected, since others studies with finer spatial resolution sensors such as Landsat-TM (Chuvieco et al., 2002) have reported lower correlations for NDVI than for NIR/SWIR indices. Therefore, our results might be due to LAI or border effects present in the coarse spatial resolution of MODIS. Lower than expected correlations for NDWI as computed from MODIS/Terra band 5, should be caused by the radiometric problems of this sensor that have been reported by several authors (Stow et al., 2005).

Table 4 – Multiple regression results for FMC estimations based on empirical data (calibration set)

Sample	Grassland					Shrubland					
	r ²	a	b ₁ (NDVI)	S.E.	n	r ²	a	b ₁ (VARI)	b ₂ (GVMi)	S.E.	n
0	0.907	-161.112	650.226	30.1	40	0.732	229.14	887.155	-300.751	17.5	40
1	0.870	-131.144	564.230	40.2	35	0.734	1,91,474	719.134	-216.348	13.3	42
2	0.879	-134.729	552.872	31.4	41	0.757	199.962	796.292	-222.873	15.9	35
3	0.845	-137.591	566.349	36.3	39	0.671	200.868	768.924	-234.900	18.1	41

Table 5 – Multiple regression results for FMC estimations based on RTM simulated data (calibration set)

Sample	Grassland						Shrubland					
	r^2	a	b_1 (LAI)	b_2 (NDII)	n	S.E.	r^2	a	b_1 DM	b_2 (GVMI)	S.E.	n
0	0.894	-6.74	131.41	296.751	1331	29.5	0.842	200.27	-5322.81	92.28	12.6	503
1	0.898	3.013	121.82	324.708	817	29.2	0.852	205.23	-5471.86	90.19	12.4	304
2	0.904	-7.746	132.31	287.376	792	29	0.844	203.161	-5472.86	96.46	12.7	298
3	0.897	-4.587	129.08	309.865	782	29.1	0.823	198.828	-5279.85	92.28	12.9	293

640

Table 6 – Results of the validation of the models (validation set)

	Empirical data					Simulated data				
	r^2	Slope	RMSE (%)	RMSEs (%)	RMSEu (%)	r^2	Slope	RMSE (%)	RMSEs (%)	RMSEu (%)
Grassland	0.9140	0.93	28.39	10.24	25.39	0.9268	0.92	24.57	8.69	22.99
Shrubland	0.7226	0.91	16.01	3.23	15.68	0.7034	0.56	25.18	19.17	10.10

625

640

According to the previous analysis, regression models based on empirical data selected different variables to those based on simulated data. The former fittings tended to select indices based on the red/NIR space, such as NDVI or VARI, while the latter chose indices in the NIR/SWIR space, such as the NDII or GVMI for grasslands or shrublands, respectively. The reason for that should be related to the indirect effects of water content variations on plant physiological activity. VARI or NDVI do not include bands with water absorption features, but they were selected in the empirical models because they are very sensitive to chlorophyll and LAI variations, which follow leaf drying in many species, and particularly in grasslands (Nelson, 2001). These indirect effects are not so evident for shrublands (Nuñez Olivera, 1988), and therefore the empirical models selected also indices including SWIR

bands, such as the GVMI. This index was also selected by the simulation model, since it is well adapted to water absorption features. In fact, it was initially designed as a water content index (Ceccato et al., 2002), although it was intended for estimation of EWT (water per leaf area), and not for FMC (water per dry mass). However, with empirical data, the most explicative index was the VARI, which is a combination of blue, green and red reflectance, as it is proposed to estimate chlorophyll content of the upper canopy. The importance of VARI for FMC was also observed by other authors working in Mediterranean shrubs (Roberts et al., 2006; Stow et al., 2005).

641

642

643

644

645

646

647

648

649

650

651

652

653

654

655

656

657

658

659

660

661

662

663

664

665

666

667

668

669

670

671

672

673

674

675

676

677

678

679

680

681

682

NDII and GVMI, NIR/SWIR indexes, are selected in models based on simulation data. Red/NIR indices were not chosen because the indirect effects of water content on chlorophyll variations were not considered in the simulations, since the chlorophyll content was fixed. Chlorophyll content decrease with water deficit in *C. ladanifer* L., following an annual cycle with higher values in winter, lower in summer and intermediate in spring and autumn (Nuñez-Olivera et al., 1996; Gratani and Varone, 2004). The reason behind selecting a fixed chlorophyll value in the simulation was, that spring chlorophyll content can be attenuated under severe drought periods what can lead to slighter differences between spring and summer values (Valladares, personal communication). Years 2004 and 2005 were specially dry in our study site (Garcia, 2007), therefore average chlorophyll values for spring and summer were not significantly different (ANOVA, $p > 0.05$). Late spring is the period of maximum leaf shedding in *C. ladanifer* L., and hence mature leaves sampled during those days showed the relatively low chlorophyll content typical of senescent leaves (Nuñez-Olivera et al., 1996). Regarding grasslands, Billore and Mall (1976) found a clear bell-shape curve in chlorophyll content, with the peak just after the rain season, so more variations in chlorophyll content are likely to be found between spring and summer. Future work should be done to consider these variations in the grassland simulations and see if the models derived changes the tendency to choose indices including SWIR bands towards Red/NIR.

LAI variations were included in the grassland model, which is indirectly related to variations of red/NIR reflectance.

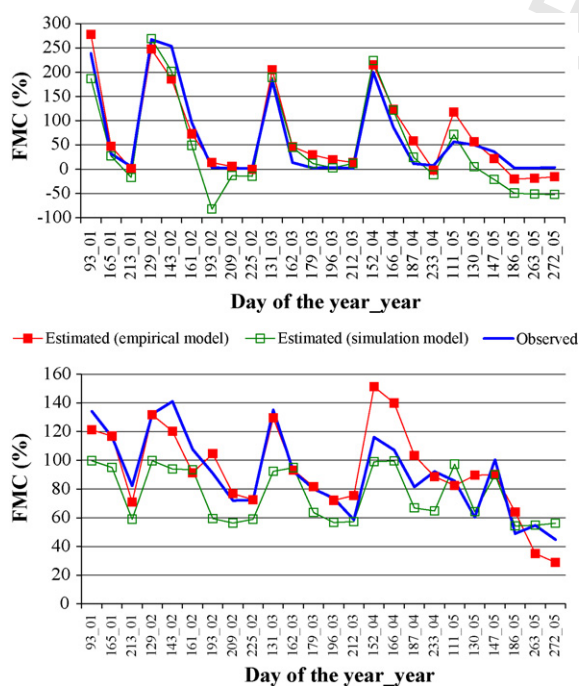


Fig. 6 – Temporal trends of FMC observed and estimated by both empirical and simulation models for grasslands (top) and shrublands (bottom).

Table 7 – Summary of advantages and disadvantages of empirical and simulated data in FMC estimation

	Simulated data	Empirical data
Calibration difficulty	High (requires detailed parameterization)	Low
Time to generate the model	High	Medium
Cost	Medium (reduces field sampling, but increases input variables that should be measured to parametrize the model)	High (intense field sampling)
Indices selected	NIR–SWIR space	Red–NIR space
Auxiliary data	High (Sun-Illumination Angles, LAI, DM, etc.)	Low (reflectance)
Robustness	High	Medium
Accuracy	Largely depend on range of input conditions and model assumptions	Largely depends on time series and spatial representativity of the sample

LAI and DM as external variables were introduced in the simulation data model based on the rules used to avoid unrealistic combinations and previous experience with RTM inversion software (Rueda, 2001), which only offered good results when LAI and DM were fixed. In this way the final simulated derived models account for variation in these two parameters.

Both modeling approaches provided good estimations of grasslands and shrublands FMC, but those based on simulated data offered a lower standard error. Negative estimations of the grassland models were not considered a serious problem, since they occurred with actual FMC values below 30%, where these fuels can be considered as dead fuels (Nelson, 2001). In integrated systems of fire risk indices, the dead FMC estimation is carried out by means of meteorological indices, therefore, a filter could avoid these negative estimations to address this error. Therefore, the model based on simulated data should be considerable more suitable because it has a tendency to under-estimate FMC whereas the empirical model over-estimate FMC in the driest periods. From the fire prevention point of view, over-estimation is considered less desirable since it would tend to reduce the fire risk rating, although false alarms are also undesirable.

Some problems with the model derived from simulated data, especially those related to shrublands estimation, might be improved with the use of a wider range of parameters, or other inversion strategies, that will be considered in the near future. Additionally, new RTM better adapted to forested areas, such as geometrical or mixed geometrical-turbid medium models, such as GORT, DART, GEOSAIL (Pinty et al., 2004), may provide better inversion in shrublands as well as extending our efforts to tree-covered areas. The generalizing power of these simulation models remains to be proven, by extending the validation sample to other study areas, which we will also plan to perform in the near future.

5. Conclusions

Developing an operational methodology of FMC estimation is a key factor for fire risk assessment. Remote sensing offers operational tools to monitor this FMC evolution. The first results that compare the effectiveness of FMC estimations from empirical methods and those based on simulated data for two representative vegetation types (Mediterranean grassland and shrublands) were covered in this paper. The model based on empirical data offered reasonable results and it was

easy to compute. The model based on simulation data, was more complex to generate, but proved more robust when several calibration samples were selected.

Further studies should test whether these models are applicable in other sites with similar environmental characteristics.

Uncited reference

Núñez-Olivera and Escudero García (1990).

Acknowledgements

This research has been funded by the Firemap project (CGL2004-060490C04-01/CLI) and the Spanish Ministry of Education and Science by means of the FPU grant program which supports Marta Yebra. We would like to give special thanks to the authorities of the Cabañeros National Park and a large list of colleagues involved in the fieldwork. Suggestions and comments from Seth Peterson of UC Santa Barbara, Mark Danson of the University of Salford, Fernando Valladares (Centro de Ciencias Medioambientales, C.S.I.C.) and two anonymous reviewers are also acknowledged.

REFERENCES

- Ahern, F.J., Goldammer, J.G., Justice, C.O. (Eds.), 2001. Global and Regional Vegetation Fire Monitoring from Space: Planning a Coordinated International Effort. SPB Academic Publishing, The Hague, The Netherlands.
- Baeza, M.J., Luis, M.D., Raventos, J., Escarre, A., 2002. Factors influencing fire behaviour in shrublands of different stand ages and the implications for using prescribed burning to reduce wildfire risk. *J. Environ. Manage.* 65, 199–208.
- Billore, S.k., Mall, L.P., 1976. Seasonal variation in chlorophyll content of a grassland community. *Trop. Ecol.* 17, 39–44.
- Blackmarr, W.H., Flanner, W.B., 1968. Seasonal and Diurnal Variation in Moisture Content of Six Species of Pocosin Shrubs. SE-33, Southeastern Forest Experiment Station. U.S. Forest Service, Asheville.
- Bowyer, P., Danson, F.M., 2004. Sensitivity of spectral reflectance to variation in live fuel moisture content at leaf and canopy level. *Remote Sens. Environ.* 92, 297–308.
- Boyer, J.S., 1995. *Measuring the Water Status of Plants and Soils.* Academic Press, INC, p. 178.

- 765
766 Burgan, R.E., Klaver, R.W., Klaver, J.M., 1998. Fuel models and
767 fire potential from satellite and surface observations. *Int. J.*
768 *Wildland Fire* 8 (3), 159–170. 834
- 769 Camia, A., Bovio, G., Aguado, I., Stach, N., 1999. Meteorological
770 fire danger indices and remote sensing. In: Chuvieco, E.
771 (Ed.), *Remote Sensing of Large Wildfires in the European*
772 *Mediterranean Basin*. Springer-Verlag, Berlin, pp. 39–59. 835
- 773 Ceccato, P., Flasse, S., Tarantola, S., Jacquemoud, S., Grégoire,
774 J.M., 2001. Detecting vegetation leaf water content using
775 reflectance in the optical domain. *Remote Sens. Environ.* 77,
776 22–33. 836
- 777 Ceccato, P., Gobron, N., Flasse, S., Pinty, B., Tarantola, S., 2002.
778 Designing a spectral index to estimate vegetation water
779 content from remote sensing data. Part 1 Theoretical
780 approach. *Remote Sens. Environ.* 82, 188–197. 837
- 781 Chen, D., 2005. Vegetation water content estimation for corn
782 and soybeans using spectral indices derived from MODIS
783 near- and short-wave infrared bands. *Remote Sens.*
784 *Environ.* 98, 225–236. 838
- 785 Chuvieco, E., Aguado, I., Cocero, D., Riaño, D., 2003a. Design of
786 an empirical index to estimate fuel moisture content from
787 NOAA–AVHRR analysis in forest fire danger studies. *Int. J.*
788 *Remote Sens.* 24 (8), 1621–1637. 839
- 789 Chuvieco, E., Allgöwer, B., Salas, F.J., 2003b. Integration of
790 physical and human factors in fire danger assessment. In:
791 Chuvieco, E. (Ed.), *Wildland Fire Danger Estimation and*
792 *Mapping: The Role of Remote Sensing Data*. World Scientific
793 Publishing, Singapore, pp. 197–218. 840
- 794 Chuvieco, E., Cocero, D., Aguado, I., Palacios-Orueta, A., Prado,
795 E., 2004a. Improving burning efficiency estimates through
796 satellite assessment of fuel moisture content. *J. Geophys.*
797 *Res.-Atmos.* 109 (D14S07), 1–8, doi:10.1029/2003JD003467. 841
- 798 Q3 Chuvieco, E., et al., 2004b. Combining NDVI and surface
799 temperature for the estimation of live fuel moisture content
800 in forest fire danger rating. *Remote Sens. Environ.* 92, 322–
801 331. 842
- 802 Chuvieco, E., Riaño, D., Aguado, I., Cocero, D., 2002. Estimation
803 of fuel moisture content from multitemporal analysis of
804 Landsat Thematic Mapper reflectance data: applications in
805 fire danger assessment. *Int. J. Remote Sens.* 23 (11), 2145–
806 2162. 843
- 807 Combal, B., et al., 2002. Retrieval of canopy biophysical
808 variables from bidirectional reflectance using prior
809 information to solve the ill-posed inverse problem. *Remote*
810 *Sens. Environ.* 84, 1–15. 844
- 811 Datt, B., 1999. Remote sensing of water content in eucalyptus
812 leaves. *Aust. J. Bot.* 47, 909–923. 845
- 813 Doerr, S.H., et al., 2006. Effects of differing wildfire severities on
814 soil wettability and implications for hydrological response.
815 *J. Hydrol.* 319, 295–311. 846
- 816 Fang, H., Liang, S., 2003. Retrieving leaf area index with a neural
817 network method: simulation and validation. *IEEE Trans.*
818 *Geosci. Remote Sens.* 41 (9), 2052–2062. 847
- 819 Fosberg, M.A., Schroeder, M.J., 1971. *Fine Herbaceous Fuels in*
820 *Fire Danger Rating*, USDA, Forest Service, Rocky Mountain
821 *Forest and Range Experiment Station*. Fort Collins,
822 Colorado. 848
- 823 Fourty, T., Baret, F., 1997. Vegetation water and dry matter
824 contents estimated from top-of-the-atmosphere reflectance
825 data: a simulation study. *Remote Sens. Environ.* 61,
826 34–45. 849
- 827 Gao, B.C., 1996. NDWI: a normalized difference water index for
828 remote sensing of vegetation liquid water from space.
829 *Remote Sens. Environ.* 58, 257–266. 850
- 830 Q4 Garabedian, P., 1964. *Partial differential equations*. 851
- 831 Garcia, M., 2007. Estimación y cartografía del contenido de
832 humedad del combustible vivo a partir de imágenes NOAA/
833 AVHRR. Departamento de Geografía, Universidad de Alcalá,
834 Alcalá de Henares. 852
- 835 Gitelson, A., Kaufman, J.Y., Stark, R., Rundquist, D., 2002. Novel
836 algorithms for remote estimation of vegetation fraction.
837 *Remote Sens. Environ.* 80, 76–87. 853
- 838 Gobron, N., et al., 2000. Potential of multiangular spectral
839 measurements to characterize land surfaces: conceptual
840 approach and exploratory application. *J. Geophys. Res.* 105
841 (D13), 17539–17549. 854
- 842 Gratani, L., Varone, L., 2004. Leaf key traits of *Erica arborea* L.,
843 *Erica multiflora* L. and *Rosmarinus officinalis* L. co-occurring in
844 the Mediterranean maquis. *Flora* 199, 56–69. 855
- 845 Huete, A.R., 1988. A soil-adjusted vegetation index (SAVI).
846 *Remote Sens. Environ.* 25, 295–309. 856
- 847 Huete, A., et al., 2002. Overview of the radiometric and
848 biophysical performance of the MODIS vegetation indices.
849 *Remote Sens. Environ.* 83 (1/2), 195–213. 857
- 850 Hunt, E.R., Rock, B.N., 1989. Detection of changes in leaf water
851 content using near and middle-infrared reflectances.
852 *Remote Sens. Environ.* 30, 43–54. 858
- 853 Jacquemoud, S., Baret, F., 1990. PROSPECT: a model of leaf
854 optical properties spectra. *Remote Sens. Environ.* 34,
855 75–91. 859
- 856 Jacquemoud, S., Ustin, S.L., 2003. Application of radiative transfer
857 models to moisture content estimation and burned land
858 mapping. In: Chuvieco, E., Martín, M.P. (Eds.), *Proceedings*
859 *of the Fourth International Workshop on Remote*
860 *Sensing and GIS Applications to Forest Fire Management:*
861 *Innovative Concepts and Methods*. University of Ghent,
862 Ghent pp. 1–10. 863
- 863 Johnson, E.A., Miyanishi, K., 2001. *Forest Fires: Behavior and*
864 *Ecological Effects*, vol. xvii. Academic Press, San Diego,
865 Calif, 594 pp. 866
- 866 Knyazikhin, Y., et al., 1999. MODIS leaf area index (LAI) and
867 fraction of photosynthetically active radiation absorbed by
868 vegetation (FPAR) product (MOD15). Algorithm Theoretical
869 Basis Document. [http://eospsso.gsfc.nasa.gov/atbd/
870 modistables.html](http://eospsso.gsfc.nasa.gov/atbd/modistables.html). 871
- 871 Lawson, B.D., Hawkes, B.C., 1989. Field evaluation of moisture
872 content model for medium-sized logging slash. In:
873 *Proceedings of the 10th Conference on Fire and Forest*
874 *Meteorology*. Ottawa, Canada pp. 247–257. 875
- 875 Leone, V., et al., 2003. The human factor in fire danger
876 assessment. In: Chuvieco, E. (Ed.), *Wildland Fire Danger*
877 *Estimation and Mapping. The Role of Remote Sensing Data:*
878 *Series in Remote Sensing*, vol. 4. World Scientific Publishing,
879 Singapore, pp. 143–196. 880
- 880 Liang, S., 2004. *Quantitative Remote Sensing for Land Surface*
881 *Characterization*, vol. xxvi. Wiley, Hoboken, NJ, 534 pp. 882
- 882 Naveh, Z., 1989. Fire in the Mediterranean: a landscape
883 ecological perspective. In: Goldammer, J.G., Jenkins, M.J.
884 (Eds.), *Proceedings of the Third International Symposium*
885 *on Fire Ecology: Fire in Ecosystem Dynamics*. SPB Academic
886 Publishing, Freiburg, Germany, pp. 1–20. 887
- 887 Nelson, R.M., 2001. Water relations of forest fuels. In: Johnson,
888 E.A., Miyanishi, K. (Eds.), *Forest Fires: Behavior and*
889 *Ecological Effects*. Academic Press, San Diego, Calif, pp. 79–
890 149. 891
- 891 Nuñez Olivera, E., 1988. *Ecología del jaral de Cistus ladanifer*,
892 *Universidad de Extremadura*. 893
- 893 Núñez-Olivera, E., Escudero García, J.C., 1990. Índice de
894 esclerofilia, área media foliar y contenido de clorofilas en
895 hojas maduras de “*Cistus ladanifer*” L. *Variaciones*
896 *estacionales*, vol. VII. *Studia Oecológica*, pp. 63–75. 897
- 897 Nuñez-Olivera, E., Martínez-Abaiar, J., Escudero, J.C., 1996.
898 Adaptability of leaves of *Cistus ladanifer* to widely varying
899 environmental conditions. *Funct. Ecol.* 10 (5), 636–646. 900
- 900 Palacios-Orueta, A., Chuvieco, E., Parra, A., Carmona-Moreno,
901 C., 2005. Biomass burning emissions: a review of models
902 using remote-sensing data. *Environ. Monit. Assess.* 104
903 (1/3), 189–209. 904

- 904 Paltridge, G.W., Barber, J., 1988. Monitoring grassland dryness
905 and fire potential in Australia with NOAA/AVHRR data.
906 *Remote Sens. Environ.* 25, 381–394.
- 907 Pinty, B., Verstraete, M.M., 1992. GEMI: a non-linear index to
908 monitor global vegetation from satellites. *Vegetation* 101,
909 15–20.
- 910 Pinty, B., et al., 2004. Radiation transfer model intercomparison
911 (RAMI) exercise: results from the second phase. 109(D6),
912 D06210. doi:10.1029/2003JD004252.
- 913 Pompe, V., Vines, R.G., 1966. The influence of moisture on the
914 combustion of leaves. *Aust. Forest.* 30, 231–241.
- 915 Qi, J., Kerr, Y., Chehbouni, A., 1994. External factor consideration
916 in vegetation index development. In: ISPRS (Eds.), *Physical
917 Measurements and Signatures in Remote Sensing.* pp. 723–
918 730.
- 919 Riaño, D., Vaughan, P., Chuvieco, E., Zarco-Tejada, P., Ustin, S.L.,
920 2005. Estimation of fuel moisture content by inversion of
921 radiative transfer models to simulate equivalent water
922 thickness and dry matter content: analysis at leaf and
923 canopy level. *IEEE Trans. Geosci. Remote Sens.* 43 (4), 819–
924 826.
- 925 Roberts, D.A., Peterson, S., Dennison, P.E., Sweeney, S., Rechel,
926 J., 2006. Evaluation of airborne visible/infrared imaging
927 spectrometer (AVIRIS) and moderate resolution imaging
928 spectrometer (MODIS) measures of live fuel moisture and
929 fuel condition in a shrubland ecosystem in southern
930 California. *J. Geophys. Res.* 111, G04S02, doi:10.1029/
931 2005JG000113.
- 932 Rouse, J.W., Haas, R.W., Schell, J.A., Deering, D.H., Harlan, J.C.,
933 1974. Monitoring the Vernal Advancement and
934 Retrogradation (Greenwave Effect) of Natural Vegetation.
935 NASA/GSFC, Greenbelt, MD, USA.
- 936 Rueda, C.A., 2001. *GSTARS Radiative Transfer Model Repository*
937 Project. Davis.
- 938 Saich, P., Lewis, P., Disney, M.I., 2003. Biophysical parameter
939 retrieval from forest and crop canopies in the optical and
940 microwave domains using 3D models of canopy structure.
941 In: *Geoscience and Remote Sensing Symposium. IGARSS
942 '03.* IEEE International, Toulouse, pp. 3546–3548.
- 943 Sepulcre-Canto, G., et al., 2006. Detection of water stress in an
944 olive orchard with thermal remote sensing imagery. *Agric.
945 Forest Meteorol.* 136 (1), 31–44.
- SPSS, 2004. *SPSS Base Users Guide.* SPSS Inc.. 945
- Stow, D., Nipahadkar, M., Kaiser, J., 2005. MODIS-derived visible
946 atmospherically resistant index for monitoring
947 chaparral moisture content. *Int. J. Remote Sens.* 26 (17),
948 3867–3873. 949
- Trowbridge, R., Feller, M.C., 1988. Relationships between the
950 moisture content of fine woody fuels in lodgepole pine slash
951 and the fine fuel moisture code of the canadian forest fire
952 weather index system. *Can. J. Forest Res.* 18, 128–131. 953
- Valladares, F., 2004. *Ecología del bosque mediterráneo en un
954 mundo cambiante.* Ministerio de Medio Ambiente. EGRAF,
955 S.A, Madrid. 956
- Vega-Garcia, C., Chuvieco, E., 2006. Applying local measures of
957 spatial heterogeneity to Landsat-TM images for predicting
958 wildfire occurrence in Mediterranean landscapes.
959 *Landscape Ecol.* 21 (4), 595–605. 960
- Verhoef, W., 1984. Light scattering by leaf layers with
961 application to canopy reflectance modeling: the SAIL model.
962 *Remote Sens. Environ.* 16, 125–141. 963
- Vermote, E.F., Vermeulen, A., 1999. Atmospheric correction
964 algorithm: spectral reflectances (MOD09). NASA. 965
- Viegas, D.X., Piñol, J., Viegas, M.T., Ogaya, R., 2001. Estimating
966 live fine fuels moisture content using meteorologically-
967 based indices. *Int. J. Wildland Fire* 10, 223–240. 968
- Viegas, D.X., Viegas, T.P., Ferreira, A.D., 1992. Moisture content
969 of fine forest fuels and fire occurrence in central Portugal.
970 *Int. J. Wildland Fire* 2 (2), 69–85. 971
- Wellburn, A.R., 1994. The spectral determination of chlorophylls
972 a and b, as well as total carotenoids, using various solvents
973 with spectrophotometers of different resolution. *J. Plant
974 Physiol.* 144, 307–313. 975
- Willmott, C.J., 1982. Some comments on the evaluation of model
976 performance. *Bull. Am. Meteorol. Soc.* 63, 1309–1313. 977
- Yebra, M., de Santis, A., Chuvieco, E., 2005. Estimación del
978 peligro de incendios a partir de teledetección y
979 variables meteorológicas: variación temporal del
980 contenido de humedad del combustible. *Recursos Rurais* 1,
981 9–19. 982
- Zarco-Tejada, P.J., Rueda, C.A., Ustin, S.L., 2003. Water content
983 estimation in vegetation with MODIS reflectance data and
984 model inversion methods. *Remote Sens. Environ.* 85,
985 109–124. 986
- 987